

# Two dimension MDW OCDMA code cross-correlation for reduction of phase induced intensity noise

Israa Sh. Ahmed<sup>1</sup>, Syed A. Aljunid<sup>2</sup>, Junita M. Nordin<sup>1</sup>, Layth A. Khalil Al Dulaimi<sup>2</sup>, Rima Matem<sup>1</sup>

<sup>1</sup> Center of Excellent Advanced Communication Engineering, School of Computer & Communication Engineering, Universiti Malaysia Perlis (UniMAP), 01000 Kangar, Perlis.

<sup>2</sup> Embedded Networking and Advance Computing Cluster, School of Computer & Communication Engineering, Universiti Malaysia Perlis (UniMAP) Tingkat 1, Kampus Tetap Pauh, Putra 02600 Arau, Perlis.

**Abstract.** In this paper, we first review 2-D MDW code cross correlation equations and table to be improved significantly by using code correlation properties. These codes can be used in the synchronous optical CDMA systems for multi access interference cancellation and maximum suppress the phase induced intensity noise. Low  $P_{sr}$  is due to the reduction of interference noise that is induced by the 2-D MDW code PIIN suppression. High data rate causes increases in BER, requires high effective power and severely deteriorates the system performance. The 2-D W/T MDW code has an excellent system performance where the value of PIIN is suppressed as low as possible at the optimum  $P_{sr}$  with high data bit rate. The 2-D MDW code shows better tolerance to PIIN in comparison to others with enhanced system performance. We prove by numerical analysis that the PIIN maximally suppressed by MDW code through the minimizing property of cross correlation in comparison to 2-D PDC and 2-D MQC OCDMA code.scheme systems.

## 1. Introduction

Codes with low cross correlation are required in spectral-amplitude-coding Optical Code Division Multiple Access (CDMA) systems since these codes eliminate multi access interference and also suppress the effect of phase-induced intensity noise. However, little research work has been done on such codes although codes with ideal low cross correlation have been studied for many years [1]. Nevertheless, in spectral-amplitude-coding systems, the inherent phase-induced intensity noise (PIIN) and many others affect the whole system performance. PIIN is due to the spontaneous emission of the broadband source, and its effect is proportional to the power of the created photocurrent [2]. Thus, the summation of different users' signals at the receiver's end fluctuates in intensity, which increases the variance of the received signal [3].

To suppress it, the value of should be kept as minor as possible. Therefore, the codes with low cross correlation become attractive. However, the performance is still limited by PIIN [4]. Earlier studies have used various methods to reduce PIIN in SAC-OCDMA systems. Some researchers have reduced the number of MAI to minimize the in-phase cross-correlation. Others have attempted different approaches in solving the problem, such as using saturated semiconductor optical amplifiers (SOA) in the noise-cleaning process [6]. Newly, the authors have proposed the modified-AND subtraction detection technique to overcome the impact of PIIN and

MAI in incoherent SAC-OCDMA systems by dividing the spectrum of the utilized code sequences at the decoder branch [6].

Optical code-division numerous entry (OCDMA) is a guaranteeing method to bursty movement network, What's more, it gives asynchronous and security transmissions the middle of different clients [7]. "around various sorts of OCDMA schemes, incoherent frameworks need to be pulled in more consideration over sound ones, because of simpler acknowledgment about encoders Furthermore decoders. However, since those embraced 1-D optical code sequences would unipolar over incoherent systems, those code length ought to make made large will hold preferred auto- What's more cross-correlations[8].

Therefore, 2-D codes need aid recommended should get great correlation aspects for short code length by using other dimensions, for example, such that wavelength, space, thus. Some writers produce 2-D optical codes by creating specific calculations [9] alternately bringing focal point of the maturely produced 1-D optical codes clinched alongside a joined time-spreading also frequency-hopping plan. These codes bring huge cardinality, yet the lengths from claiming fiber delay lines utilized within the coding units would very much longer, Also multiple-access impedance (MAI).

\* Corresponding author: israashihab83@gmail.com

## 2. Review of 2-D MDW Code Cross Correlation

The 2-D W/T MDW OCDMA synchronous number of clients is dictated by the duplication of wavelengths  $M$  and time—chips  $N$ . All in all, an expanded number of clients results in an extension in code length, effective power, reducing the bit rate, the increment in impedance acquainted with the framework which causes framework decay. The number of Hamming weight or code weight ( $W$ ) depends on the size of the chosen codes. High Hamming weight of "1", in the code sequence, indicates an increase in short optical pulses scattered along the spectrum. The size of the code is indicated by the code length indicator. Usually, high code size will result in an increase in code length [8]. A good code sequence should have high code sequences, reasonable code length, low code weight and BER below  $10^{-9}$  error floor. Bit rate or data rate is a measure of a number of bits transmitted per second over a fiber channel. Bit rate reflects the information carrying capacity of a fiber communications link. High data rate will increase the BER and deteriorate the system performance. Noise power is the noise interference that exists in the system other than the desired signal. The wavelength-time code cross-correlation is generated differently compared to the 1-D OCDMA code [9].

Let;

$$X = [x_0, x_1, x_2, \dots, x_{M-1}]$$

$Y = [y_0, y_1, y_2, \dots, y_{N-1}]$ , be the code sequence of the 2-D MDW OCDMA code.

The cross-correlation of 2-D W/T MDW can be developed by proffering the four characteristic matrices of  $A^{(d)}$ , where  $d$  is the subset of 0,1,2 or 3,  $d \in \{1,2,3\}$ , are defined as:

$$A^{(0)} = Y^T X, A^{(1)} = Y^T \bar{X}, A^{(2)} = \bar{Y} X \text{ and } A^{(3)} = \bar{Y} \bar{X}.$$

The  $\bar{X}$  and  $\bar{Y}$  are the complement of  $X = [x_0, x_1, x_2, \dots, x_{M-1}]$  and

$Y = [y_0, y_1, y_2, \dots, y_{N-1}]$  respectively. Example, if  $X$  is equal **[000011011]** the complement of  $X$  will be the complement of all elements in  $X$  which is  $\bar{X} = [111100100]$ .

The cross-correlation of 2-D W/T MDW code  $A^{(d)}$  and  $A_{g,h}$  can be represented by [10]:

$$R^{(d)}(g, h) = \sum_{i=0}^{M-1} \sum_{j=0}^{N-1} a_{ij}^{(d)} a_{(i+g)(j+h)} \quad (1)$$

**Fig.1.** Generate Cross-Correlation of 2-D W/T MDW OCDMA code for  $d = 2$ .

Where  $a_{ij}^{(d)}$  is  $(i, j)_{th}$  of  $A^{(d)}$  and  $a_{(i+g)(j+h)}$  is the element  $(i, j)_{th}$  of  $A_{g,h}$ ,  $g \in \{1,2,3, \dots, M-1\}$  and  $h \in \{1,2,3, \dots, N-1\}$ .

From Equation 1, the cross-correlation Table 1 of the code was developed. In Fig. 1 the cross-correlation which was developed for  $d$  is equal to 0;  $A^{(2)} = \bar{Y} X$ . If  $k_1 = 4$  and  $k_2 = 2$ . The complete calculation can be done by setting the following element,  $d=0, 1,2,3$ , for the example that uses  $d = 2$ . From the Equation (1) and Figure 1,  $A^{(2)} = \bar{Y} X$  where  $k_1 = 4$  and  $k_2 = 2$  it is necessary to multiply the right and the left side of the above of  $n$  Figure 1, then Table 1 of cross correlation is the result as shown.

The multiplication configuration can be simplified as follow:

$$\left. \begin{matrix} A_{1,1} \times A_{1,1} \\ A_{1,2} \times A_{1,2} \\ A_{1,3} \times A_{1,3} \\ A_{2,1} \times A_{2,1} \\ A_{2,2} \times A_{2,2} \\ A_{2,3} \times A_{2,3} \end{matrix} \right\} 0 \quad \left. \begin{matrix} A_{1,1} \times A_{1,2} \\ A_{1,1} \times A_{1,3} \\ A_{2,1} \times A_{2,3} \\ A_{2,1} \times A_{2,2} \\ A_{2,2} \times A_{2,1} \\ A_{2,3} \times A_{2,3} \end{matrix} \right\} 0$$

$$\left. \begin{matrix} A_{1,1} \times A_{2,1} \\ A_{1,2} \times A_{2,2} \\ A_{1,3} \times A_{2,3} \\ A_{2,1} \times A_{1,1} \\ A_{2,2} \times A_{1,2} \\ A_{2,3} \times A_{1,3} \end{matrix} \right\} 4 \quad \left. \begin{matrix} A_{1,1} \times A_{2,2} \\ A_{2,1} \times A_{1,2} \\ A_{1,2} \times A_{1,3} \\ A_{1,3} \times A_{2,1} \\ A_{2,3} \times A_{1,2} \\ A_{2,2} \times A_{1,1} \end{matrix} \right\} 1$$

**Table 1.** The calculation of 2-D W/T MDW code cross-correlation.

$X_{g,h}$	$R_{(g,h)}^{(2)}$	$R_{(g,h)}^{(2)}$
$g=0, h=0$	0	0
$g=0, h \neq 0$	0	0
$g \neq 0, h=0$	$k_2(k_1-1)$	4
$g \neq 0, h \neq 0$	$k_1-1$	1

Table 2 shows the derivation of the equation (1), this table is the calculation of 2-D W/T MDW code cross-correlation. A unique 2-D code cross-correlation function was generated from this table. From Table 2, the tabulated cross-correlation of 2-D W/T MDW OCDMA codes were generated from  $R^{(d)}(g, h)$  of different  $d$  values, where  $R^{(3)}(g, h)$  had a non-zero value only when  $g \neq 0 \cap h \neq 0$  and  $R^{(3)}(g, h)$  were developed. In the end, 2-D W/T MDW OCDMA cross-correlation function was derived by using  $R^{(3)}(g, h)$  to eliminate the influence due to  $A_{g,h}$  from  $R^{(0)}(g, h)$ ,  $R^{(1)}(g, h)$  and  $R^{(2)}(g, h)$ , at  $g \neq 0 \cap h \neq 0$ .

**Table 2.** Cross-Correlation of 2-D W/T MDW OCDMA code.

$X_{g,h}$	$R_{(g,h)}^{(0)}$	$R_{(g,h)}^{(1)}$	$R_{(g,h)}^{(2)}$	$R_{(g,h)}^{(3)}$
$g=0, h=0$	$k_1 k_2$	0	0	0
$g=0, h \neq 0$	$k_1$	$k_1$	0	0
$g \neq 0, h=0$	$k_2$	0	$k_2(k_1-1)$	0
$g \neq 0, h \neq 0$	1	1	$k_1-1$	$k_1-1$

The  $R^{(1)}(g, h)$  and  $R^{(2)}(g, h)$  consist of the non-zero value when  $g=0 \cap h \neq 0$ ,  $g \neq 0 \cap h=0$  respectively.

Hence, this can be used to eliminate the influence caused by  $A_{g,h}$  on  $g=0 \cap h \neq 0$ ,  $g \neq 0 \cap h=0$  from  $R^{(0)}(g, h)$  and subsequently the following equation is developed [11]:

$$R_1^{(0)}(g, h) - R_1^{(1)}(g, h) - \frac{R_1^{(2)}(g, h)}{(k_1 - 1)} = \begin{cases} k_1 k_2, \text{ for } g=0 \text{ and } h=0 \\ 0, \text{ otherwise} \end{cases} \quad (2)$$

the new 2-D W/T MDW OCDMA cross-correlation equation is developed as:

$$R^{(0)}(g, h) - R^{(1)}(g, h) - \frac{R^{(2)}(g, h)}{(k_1 - 1)} + \frac{R^{(3)}(g, h)}{(k_1 - 1)} = \begin{cases} k_1 k_2, \text{ for } g=0 \text{ and } h=0 \\ 0, \text{ otherwise} \end{cases} \quad (3)$$

This equation is used for MAI mitigation and PIIN suppression in the overall 2-D W/T MDW OCDMA code.

PIIN is the result of mixing an incoherent light field's incident which causes intensity noise at PD output []. The power of PIIN that exists in a photocurrent of the receiver can be written as [11, 12]:

$$I_{PIIN}^2 = B_r I_r^2 \tau_r = \frac{B_r \mathfrak{R}^2 P_{sr}^2}{2M\Delta f k_2^2} \left[ k_1 k_2 (MN-1)^2 + k_2 (W-1)(M-1) \right] \quad (4)$$

$$I_{thermal}^2 = \frac{4K_b T_n B_r}{R_L} \quad (5)$$

$$\begin{aligned} I_{shot}^2 &= 2eB_r(I_0 + I_1 + I_2 + I_3) \\ &= 2eB_r \frac{\mathfrak{R}^P P_{sr}}{Mk_2(MN-1)} \left\{ k_1 k_2 (MN-1) + 2k_1 (W-1)(N-1) + 2k_2 (W-1)(M-1) + 4(W-1)(M-1)(N-1) \right\} \end{aligned} \quad (6)$$

$$SNR = \frac{I_r^2}{I_{PIIN}^2 + I_{shot}^2 + I_{thermal}^2} \quad (7)$$

$$BER(M) = \frac{1}{2} \operatorname{erfc} \left( \sqrt{\frac{SNR}{8}} \right) \quad (8)$$

here  $\mathfrak{R}$  is the response of the photodiode,  $\mathfrak{R} = \eta e / hf_0$ ,  $\eta$  is the quantum efficiency of the PD,  $h$  is the Plank's constant and  $f_0$  is the central frequency of the incident light.

### 3. Results and Discussion

The In the theoretical calculation, the link parameter of the Equation (10) that has been used is shown in Table 3 These parameters are the same as used in Arief & Abdullah (2013).

**Table 3.** Parameters Used in Numerical Calculation [11].

Parameters Used in Numerical Calculation	
PD quantum efficiency	$\eta_c=0.75$
Spectral width of broadband light source	$\Delta\lambda=30\text{nm}(\Delta\lambda=3.75\text{THz})$
Operating wavelength	$\lambda_o=1.55\mu\text{m}$
Electrical bandwidth	$B=311\text{ MHz}$
Data transmission rate	$R_b =0.622\text{ Gbps, } 1.1\text{ Gbps, } 2.5\text{ Gbps and } 10\text{ Gbps.}$
Receiver noise temperature	$T_n =300\text{K}$
Receiver load resistor	$R_L=1030\Omega$
Boltzmann's constant	$K_b=1.38\times 10^{-23}\text{ W/K/Hz}$
Electron charge	$e=1.60217646\times 10^{-19}\text{ coulomb}$
Light velocity	$C=3\times 10^8\text{m/s}$

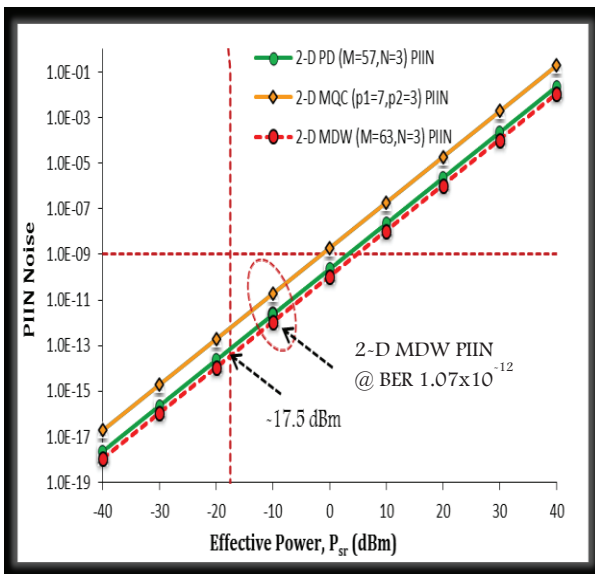


**Fig. 2.** BER PIIN noise versus effective power ( $P_{sr}$ ) for 2-D MDW ( $M=63, N=3$ ), 2-D PDC ( $M=57, N=3$ ), 2-D MQC ( $p_1=7, p_2=3$ ).

In figure 2, it observed that PIIN curves are linearly increasing at constant slope as  $P_{sr}$  expanded. The BER increases by almost two order of magnitude system performance as  $P_{sr}$  is increased by a factor of 10 dBm. From the figure which that shows 2-D MDW improves

2.15 and 17.94 folds compare to 2-D PDC and 2-D MQC and details in Table 2. 2-D MDW code successfully suppresses the PIIN results in BER at the lowest curve in comparison to 2-D PDC and 2-D MQC code. At-10 dBm below  $10^{-9}$  error floor, 2-D MDW, 2-D PDC and 2-D MQC PIIN values are  $1.08 \times 10^{-11}$ ,  $2.5 \times 10^{-13}$  and  $2 \times 10^{-11}$  respectively. Code with lowest PIIN suppression will improve the BER and overall system performance. Because of the property of cross-correlation so can achieve the optimum PIIN suppression when the  $P_{sr}$  is at -17.5 dBm .

**Table 4.** PIIN Improvement

Code	PIIN at -10.0 dBm	Improvement
2-D MDW(63x3)	$1.07 \times 10^{-12}$	2.15 and 17.94 fold smaller compare to 2-D PDC and 2-D MQC.
2-D PDC(57x3)	$2.30 \times 10^{-12}$	
2-D MQC(7x3)	$1.92 \times 10^{-11}$	

Figure 3 shows the effect of bit rate on PIIN for 2-D MDW ( $M=3, N=108$ ) at different data bit rates, 0.622 Gbps, 1.1 Gbps, 2.5 Gbps and 10 Gbps. The linear curves show an increase in PIIN noise as the data bit rate increase. Maximum PIIN suppression for low bit rate. The magnitude of PIIN system performance Suppressed by the factor of 1.3, 3.2 and 6.9 as bit rate decreases; 10.0, 5.0, 1.1 and 0.662 Gbps. High bit rate reduces total photocurrent and increases total noise power.

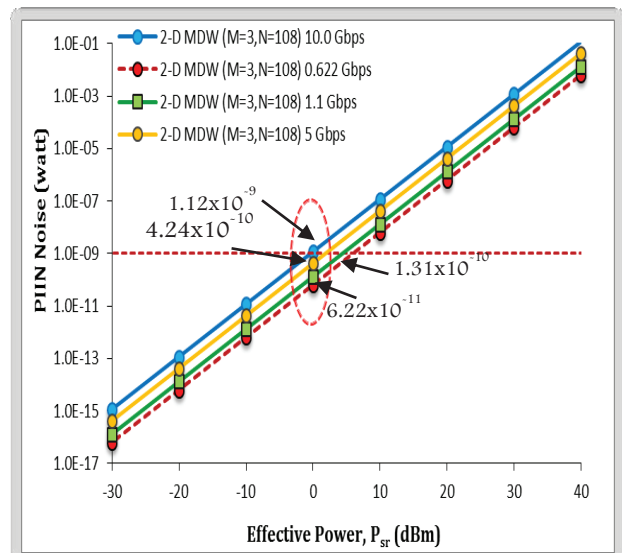


**Fig. 3.** PIIN noise versus effective power ( $P_{sr}$ ) for 2-D MDW ( $M=3, N=108$ ) at a different data rate; 0.622 Gbps, 1.1 Gbps, 2.5 Gbps and 10 Gbps.

### 4. Conclusion

Analyzing the impact of PIIN suppression on 2-D MDW OCDMA system compare to others of 2-D OCDMA

systems is done in this paper. 2-D MDW code properties improved the ability to mitigation MAI and maximally suppression of PIIN at the low optimum effective transmitted power. The property of minimum cross-correlation caused optimum PIIN suppression. PIIN is the dominant factor in 2-D MDW and others performance deterioration. However, 2-D MDW scheme has better acceptance applied to suppression PIIN. The 2-D MDW code property restrains the system degradation. Successfully suppressed PIIN by magnitude of 2.15 and 17.94 with comparison to 2-D PDC and 2-D MQC code

## References

1. J. Huang, C. Yang. IEEE Transactions on Comm. , **54** ,1, pp 150-8 (2006).
2. H. Al-Khafaji, S. Aljunid, A. Amphawan, H. Fadhil, A. Safar. Int. J. of Eng. and Tech. (IJET). **5**, 1, pp 95-100 (2013).
3. N. Keraf, S. Aljunid, A. Arief, M. Nurol, M. Anuar, C. Rashidi, P. Ehkan.. *IEEE 5th International Conference in Photonics*, p166-168 (2014).
4. H. Fathallah,, A. Bentrchia,, & H. Seleem. IET Communications, **8**(13), 2393-2403. (2014).
5. S. Panda, U. Bhanja. Int. J. of Electro. and Comm. Eng., **9**, 11, 2015
6. H. Al-Khafaji. Novel detection techniques for SAC-OCDMA system. Doctoral dissertation, Universiti Malaysia Perlis (UniMAP) (2014).
7. S. Singh. Optical Fiber Tech.. **31**;32:123-8 ( 2016).
8. I. Ahmed, S. Aljunid, C. Rashidi, L. Al Dulaimi. 3rd *International Conference Electronic Design (ICED)*, 2016 ,159-163 (2016).
9. I. Ahmed, S. Aljunid., C. Rashidi, & L. Al Dulaimi. SSRN Electronic Journal (IJCCIE), **3**,1, p73-76 (2016).
10. I. Ahmed, S. Aljunid, C. Rashidi, L. Al dulaimi.. Australian J. of Basic and Appl. Sci. **11**,1,pp 83-90 (2017).
11. A. Arief, S. AlJunid , M. Anuar , Junita M. , R. Ahmad , F. .Ghani 2012 IEEE 3rd International Conference on Electronics Design, pp.275-279 (2012).
12. A. Arief, S. AlJunid , M. Anuar , Junita M. , R. Ahmad . J International for Light and Electron Optics, **24**, 19, (2012).